22 Gecko Feet: Natural Attachment Systems for Smart Adhesion

Bharat Bhushan · Robert A. Sayer

22.1 Introduction

Almost 2500 years ago, the ability of the gecko to "run up and down a tree in any way, even with the head downwards" was observed by Aristotle [2]. This phenomenon is not limited to geckos, but occurs in several animals and insects as well. This universal attachment ability will be referred to as reversible adhesion or smart adhesion [15]. Many insects (i.e., flies and beetles) and spiders have been the subject of investigation. Geckos, however, have been the most widely studied owing to the fact that they exhibit the most versatile and effective adhesive known in nature. As a result, the vast majority of this chapter will be concerned with gecko feet.

Although there are over 1000 species of geckos [30,48], the Tokay gecko (*Gekko gecko*) has been the main focus of scientific research [34, 41]. The Tokay gecko is the second largest gecko species, attaining lengths of approximately 0.3–0.4 and 0.2–0.3 m for males and females, respectively. They have a distinctive blue or gray body with orange or red spots and can weigh up to 300 g [76]. These geckos have been the most widely investigated species of gecko owing to the availability and size of these creatures.

Even though the adhesive ability of geckos has been known since the time of Aristotle, little was understood about this phenomenon until the late nineteenth century when microscopic hairs covering the toes of the gecko were first noted. The development of electron microscopy in the 1950s enabled scientists to view a complex hierarchical morphology that covers the skin on the gecko's toes. Over the past century and a half, scientific studies have been conducted to determine the factors that allow the gecko to adhere and detach from surfaces at will, including surface structure [3, 5, 41, 59–61, 63, 80], the mechanisms of adhesion [6–8, 19, 26, 34, 39, 59, 64, 67, 73, 78], and adhesive strength [3, 6, 34, 38, 39, 41].

There is great interest among the scientific community to further study the characteristics of gecko feet in the hope that this information can be applied to the production of microsurfaces/nanosurfaces capable of recreating the adhesive forces generated by these lizards. Common man-made adhesives such as tape or glue involve the use of wet adhesives that permanently attach two surfaces. However, replication of the characteristics of gecko feet would enable the development of a superadhesive polymer tape capable of clean, dry adhesion [25,52,53,68,70,71,81]. These reusable adhesives have potential for use in everyday objects such as tape, fasteners, and toys [23] and in advanced technology such as microelectric and space applications [52, 81]. Replication of the dynamic climbing and peeling ability of geckos could find use in the treads of wall-climbing robots [51, 71].

22.2 Tokay Gecko

22.2.1 Construction of Tokay Gecko

The explanation for the adhesive properties of gecko feet can be found in the surface structure of the skin on the toes of the gecko. The skin comprises a complex fibrillar structure of lamellae (scansors), setae, branches, and spatulae [59]. As shown in Figs. 22.1 and 22.2 [4, 6, 24], the gecko consists of an intricate hierarchy of structures beginning with lamellae, soft ridges that are 1–2 mm in length [59] that are located on the attachment pads (toes) that compress easily so that contact can be made with rough bumpy surfaces. Tiny curved hairs known as setae extend from the lamellae. These setae are typically 30–130 μm in length and 5–10 μm in diameter [34, 59, 60, 80]. At the end of each seta, 100–1000 spatulae (called because of its shape) [34, 59] with a diameter of 0.1–0.2 μm [59] branch out and form the points of contact with the surface. The tips of the spatulae are approximately 0.2–0.3 μm in width [59], 0.5 μm in length, and 0.01 μm in thickness [57].

Several studies have been conducted to determine the number and size of the setae and spatulae of the gecko. Scanning electron microscopy has been employed to visually determine the values listed in Table 22.1. The setal density was originally reported to be 5000 setae per square millimeter by [59]. This value has been used in various scientific studies [6]. On the basis of pictures obtained with a scanning electron microscope (SEM), a more accurate value of about 14,000 setae per square millimeter has been proposed by [63] and verified

Table 22.1. Surface characteristics of Tokay gecko feet

	Size	Density	Adhesive force
Seta	30–130[a–d]/5–10[a–d] length/diameter (μm)	∼ 14,000[f,h] setae/mm^2	194 μN[h]
Branch	20–30[a]/1–2[a] length/diameter (μm)	–	–
Spatula	2–5[a]/0.1–0.2[a,e] length/diameter (μm)	100–1000[a,b] spatulae per seta	–
Tip of spatula	∼ 0.5[a,e]/0.2–0.3[a,d]/∼ 0.01[e] length/width/thickness (μm)	–	11 nN[i]

Young's modulus of surface material for keratin is 1–20 GPa [9, 61]
[a] [59]
[b] [34]
[c] [60]
[d] [80]
[e] [57]
[f] [63]
[g] [5]
[h] [6]
[i] [38]

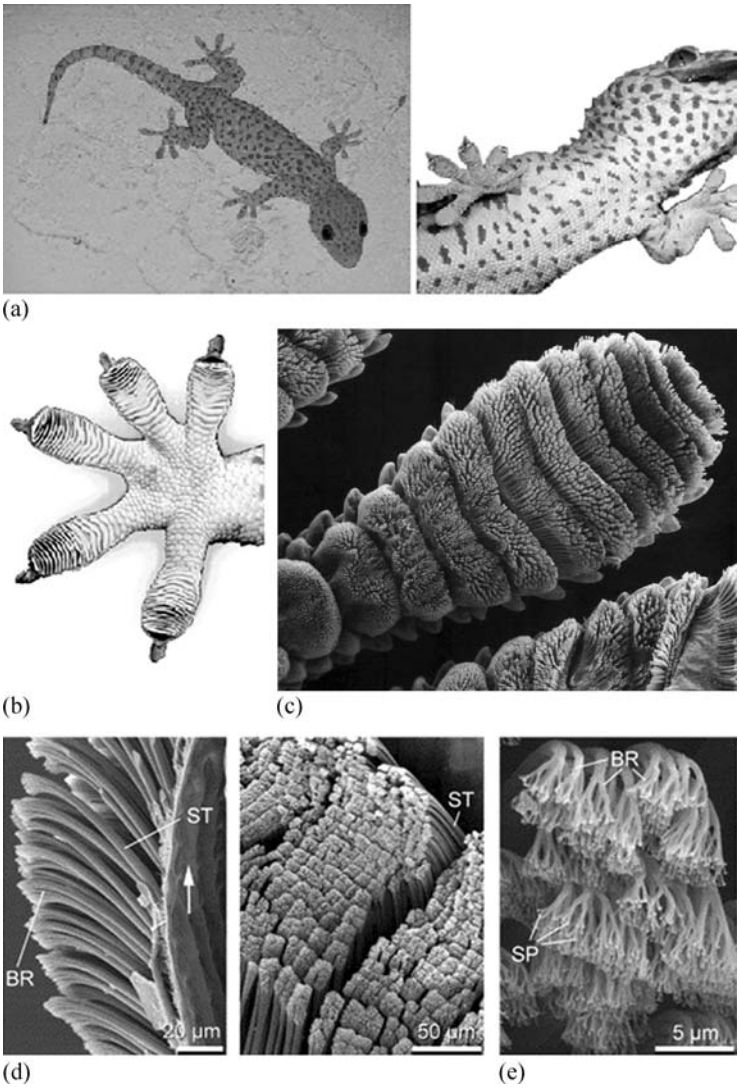

Fig. 22.1. (**a**) A Tokay gecko [6]. The hierarchical structures of a gecko foot; (**b**) a gecko foot [6] and (**c**) a gecko toe [4]. Each toe contains hundreds of thousands of setae and each seta contains hundreds of spatulae. Scanning electron microscope (SEM) micrographs of (**d**) the setae [24] and (**e**) the spatulae [24]. ST seta, SP spatula, BR branch

by [5]. The attachment pads on two feet of the Tokay gecko have an area of about 220 mm^2, which can produce a clinging ability of about 20 N, the vertical force required to pull a lizard down a nearly vertical (85°) surface [41]. In isolated setae a 2.5-µN preload yielded adhesion of 20 to 40 µN and thus the adhesion coefficient, which represents the strength of adhesion as a function of preload as 8 to 16 [7].

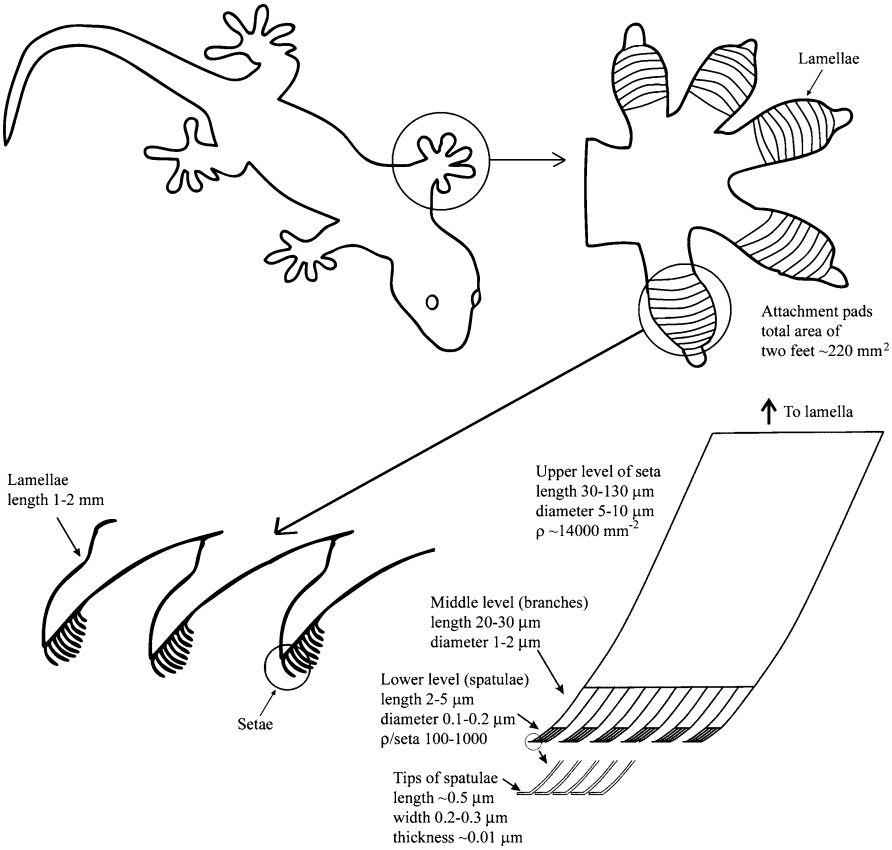

Fig. 22.2. A Tokay gecko including the overall body, one foot, a cross-sectional view of the lamellae, and an individual seta

22.2.2 Other Attachment Systems

Attachment systems in other creatures such as insects and spiders have similar structures to that of gecko skin. The microstructures utilized by beetles, flies, spiders, and geckos can be seen in Fig. 22.3a. As the size (mass) of the creature increases, the radius of the terminal attachment elements decreases. This allows a greater number of setae to be packed into an area, hence increasing the real area of contact and the adhesive strength. It was determined by [3] that the density of the terminal attachment elements, ρ_A, per square meter strongly increases with increasing body mass, m, in kilograms. In fact, a master curve can be fit between all the different species (Fig. 22.3b):

$$\log \rho_A = 13.8 + 0.669 \log m \ . \tag{22.1}$$

The correlation coefficient, r, of the master curve is equal to 0.919. Flies and beetles have the largest attachment pads and the lowest density of terminal attachment

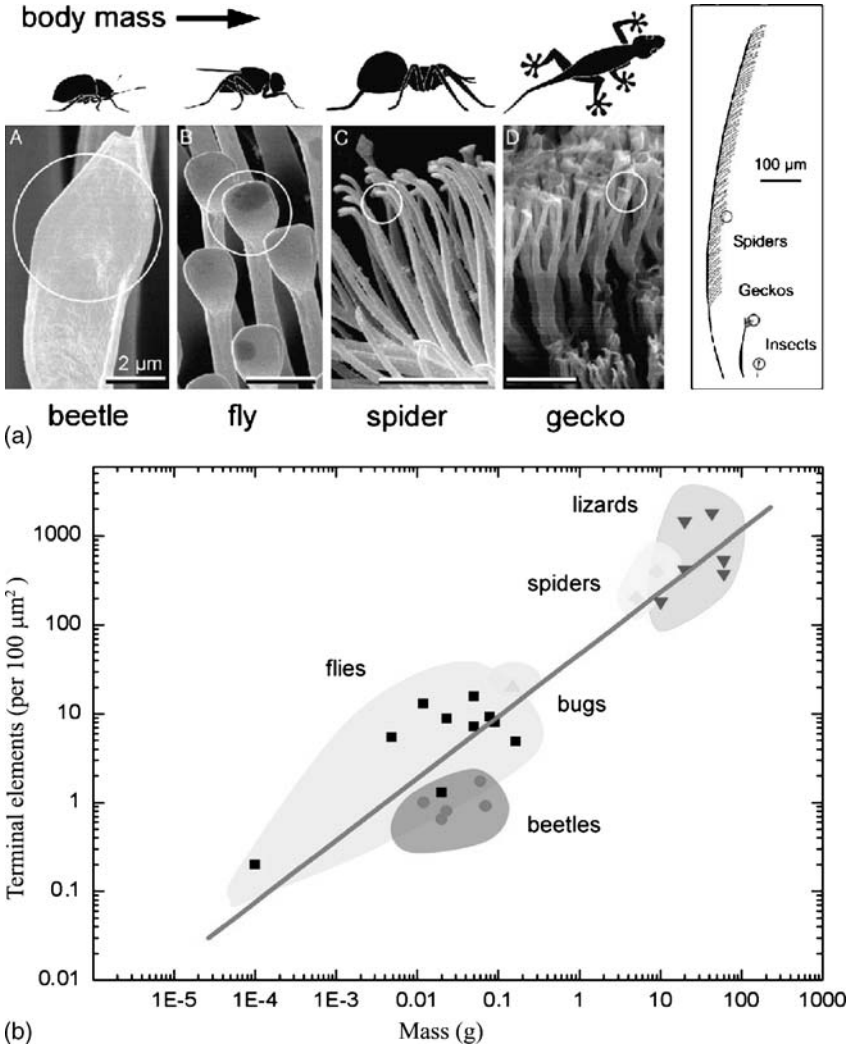

Fig. 22.3. (**a**) Terminal elements of the hairy attachment pads of a beetle, fly, spider, and gecko and (**b**) the dependence of terminal element density on body mass [3]

elements. Spiders have highly refined attachment elements that cover the leg of the spider. Lizards have both the highest body mass and the greatest density of terminal elements (spatulae).

22.2.3 Adaptation to Surface Roughness

Typical rough, rigid surfaces are only able to make intimate contact with a mating surface equal to a very small portion of the perceived apparent area of contact. In fact,

the real area of contact, A_r, is typically 2–6 orders of magnitude less than the apparent area of contact, A_a [12, 13]. Autumn et al. [7] proposed that divided contacts serve as a means for increasing adhesion. Arzt et al. [3] used a thermodynamical surface energy approach to calculate adhesive force. The authors assumed that a spatula is a hemisphere with radius R. For calculation of the adhesive force of a single contact, F_a, Johnson–Kendall–Roberts (JKR) theory was used [47]:

$$F_a = -(3/2)\,\pi\gamma R\ , \tag{22.2}$$

where γ is surface energy per unit area. Equation (22.2) shows that adhesive force of a single contact is proportional to a linear dimension of the contact. For a constant area divided into a large number of contacts or setae, n, the radius of a divided contact, R_1, is given by $R_1 = R/\sqrt{n}$; therefore, the adhesive force of (22.2) can be modified for multiple contacts such that

$$F'_a = -(3/2)\,\pi\gamma\left(R/\sqrt{n}\right)n = \sqrt{n}F_a\ , \tag{22.3}$$

where F'_a is the total adhesive force from the divided contacts. Thus, the total adhesive force is simply the adhesive force of a single contact multiplied by the square root of the number of contacts. However, this model only considers contact with a flat surface.

On natural rough surfaces the compliance and adaptability of setae are the primary sources of high adhesion. Intuitively, the hierarchical structure of gecko

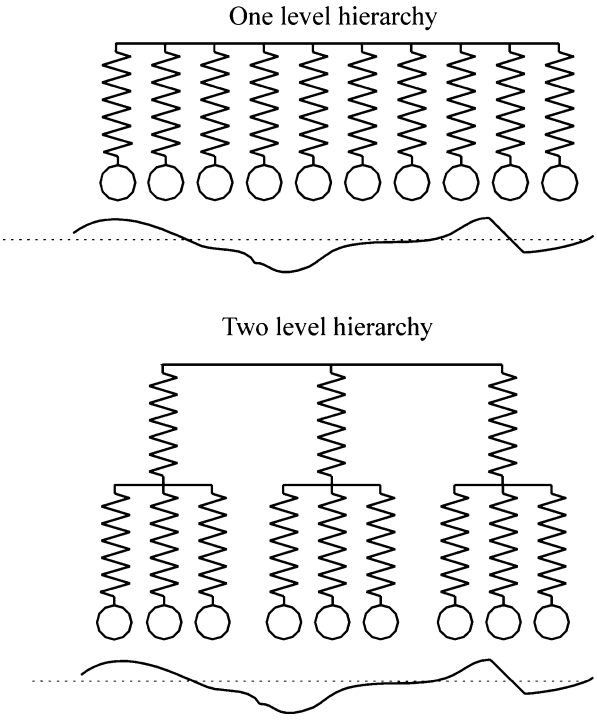

Fig. 22.4. One- and two-level spring models for the simulation of a seta of a Tokay gecko in contact and a random rough surface [15]

setae allows for greater contact with a natural rough surface than a nonbranched attachment system. Two-dimensional profiles of surfaces that a gecko may encounter were obtained using a stylus profiler. These profiles along with the surface-selection methods and surface parameters for scan lengths of 80, 400, and 2000 μm are presented in the "Appendix". Bhushan et al. [15] used the spring model of Fig. 22.4 to simulate the contact between a gecko seta and random rough surfaces similar to those found in the "Appendix". The results of this model suggest that as levels of hierarchy are added to a surface, the adaptation range to the roughness of that surface increases. The lamellae can adapt to the waviness of the surface, while the setae and spatulae allow for the adaptation to microroughness and nanoroughness, respectively. Through the use of the hierarchy of the structures of its skin, a gecko is able to bring a much larger percentage of its skin in contact with the mating surface.

Material properties also play an important role in adhesion. A soft material is able to achieve greater contact with a mating surface than a rigid material (Sect. 22.5.2). Gecko skin is composed of β-keratin, which has a Young's modulus in the range 1–20 GPa [9, 61]. Gecko setae have a Young's modulus much lower than that of the bulk material. Autumn [4] has experimentally determined that setae have an effective modulus of about 100 kPa. By combining optimal surface structure and material properties, Mother Nature has created an evolutionary superadhesive.

22.2.4 Peeling

Although geckos are capable of producing large adhesive forces, they retain the ability to remove their feet from an attachment surface at will by peeling action. Orientation of spatulae facilitates peeling. Autumn et al. [6] were the first to experimentally show that adhesive force of gecko setae is dependent on the three-dimensional orientation as well as the preload applied during attachment (Sect. 22.4.1.1). Owing to this fact, geckos have developed a complex foot motion during walking. First the toes are carefully uncurled during attachment. The maximum adhesion occurs at an attachment angle of 30° – the angle between a seta and the mating surface. The gecko is then able to peel its foot from surfaces one row of setae at a time by changing the angle at which its setae contact a surface. At an attachment angle greater than 30° the gecko will detach from the surface.

Shah and Sitti [65] determined the theoretical preload required for adhesion as well as the adhesive force generated for setal orientations of 30°, 40°, 50°, and 60° in order for a solid material (elastic modulus, E, Poisson's ratio, ν) to make contact with the rough surface described by

$$f(x) = h \sin^2\left(\frac{\pi x}{\lambda}\right) , \tag{22.4}$$

where h is the amplitude and λ is the wavelength of the roughness profile. For a solid adhesive block to achieve intimate contact with the rough surface neglecting surface forces, it is necessary to apply a compressive stress, S_c [45]

$$S_c = \frac{\pi E h}{2\left(1-\nu^2\right)\lambda} . \tag{22.5}$$

Equation (22.5) can be modified to account for fibers oriented at an angle θ. The preload required for contact is summarized in Fig. 22.5a. As the orientation angle decreases, so does the required preload. Similarly, adhesive strength is influenced by fiber orientation. As seen in Fig. 22.5b, the greatest adhesive force occurs at $\theta = 30°$.

Gao et al. [24] created a finite-element model of a single gecko seta in contact with a surface. A tensile force was applied to the seta at various angles, θ, as shown in Fig. 22.5c. For forces applied at an angle less than 30°, the dominant failure mode was sliding. In contrast, the dominant failure mode for forces applied at angles greater than 30° was detachment. This verifies the results of [6] that detachment occurs at attachment angles greater than 30°.

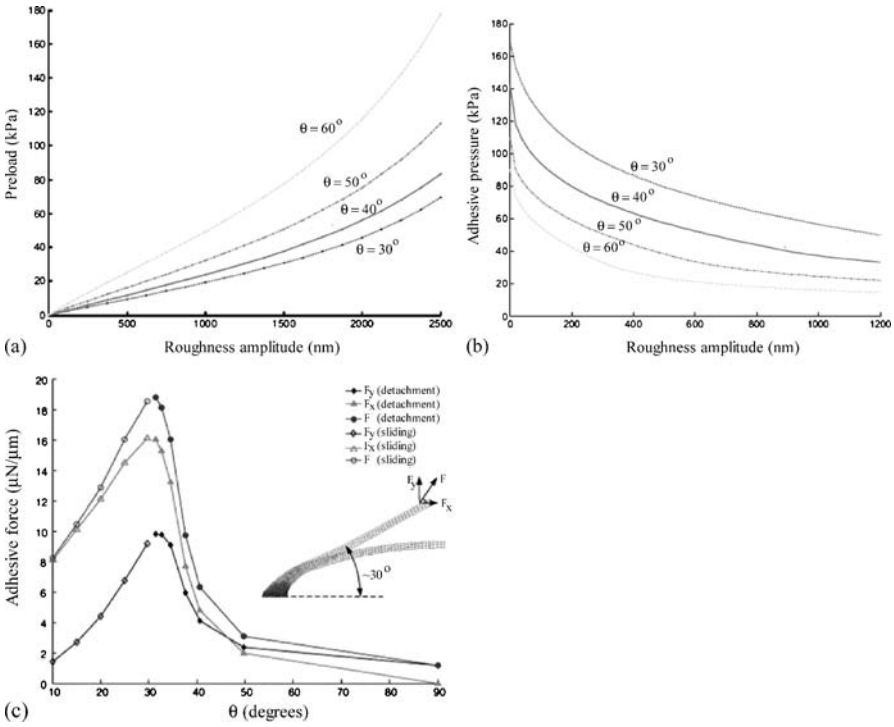

Fig. 22.5. Contact mechanics results for the effect of fiber orientation on (**a**) preload and (**b**) adhesive force for roughness amplitudes ranging from 0 to 2500 nm [65]. (**c**) Finite-element analysis of the adhesive force of a single seta as a function of pull direction [24]

22.2.5 Self-Cleaning

Natural contaminants (dirt and dust) as well as man-made pollutants are unavoidable and have the potential to interfere with the clinging ability of geckos. Par-

ticles found in the air consist of particulates that are typically less than 10 μm in diameter while those found on the ground can often be larger [35, 44]. Intuitively, it seems that the great adhesive strength of gecko feet would cause dust and other particles to become trapped in the spatulae and that they would have no way of being removed without some sort of manual cleaning action on the part of the gecko. However, geckos are not known to groom their feet like beetles [74] nor do they secrete sticky fluids to remove adhering particles like ants [22] and tree frogs [31], yet they retain adhesive properties. One potential source of cleaning is during the time when the lizards undergo molting, or the shedding of the superficial layer of epidermal cells. However, this process only occurs approximately once per month [77]. If molting were the sole source of cleaning, the gecko would rapidly lose its adhesive properties as it is exposed to contaminants in nature [32]. Hansen and Autumn [32] tested the hypothesis that gecko setae become cleaner with repeated use – a phenomenon known as self-cleaning.

The cleaning ability of gecko feet was first tested experimentally. The test procedures employed by [32] will be summarized. Silica–alumina ceramic microspheres of 2.5-μm radius were applied to clean setal arrays. Figure 22.6a shows the setal arrays immediately after dirtying and after five simulated steps. It can be noticed that a significant fraction of the particles has been removed after five steps as compared with the original dirtied arrays. The maximum shear stress that these "dirty" arrays could withstand was measured using a piezoelectric force sensor. After each step that the gecko took, the shear stress was once again measured. As seen in Fig. 22.6b, after only four steps, the gecko foot is clean enough to withstand its own body weight.

In order to understand this cleaning process, substrate–particle interactions must be examined. The interaction energy between a dust particle and a wall and spatulae can be modeled as shown in Fig. 22.7. The interaction between a spherical dust particle and the wall, W_{pw}, can be expressed as [43]

$$W_{\mathrm{pw}} = \frac{-A_{\mathrm{pw}} R_{\mathrm{p}}}{6 D_{\mathrm{pw}}} \,, \tag{22.6}$$

where p and w refer to the particle and wall, respectively. A is the Hamaker constant, R_{p} is the radius of the particle, and D_{pw} is the separation distance between the particle and the wall. Similarly, the interaction energy between a spherical dust particle and a spatula, s, assuming that the spatula tip is spherical, is [43]

$$W_{\mathrm{ps}} = \frac{-A_{\mathrm{ps}} R_{\mathrm{p}} R_{\mathrm{s}}}{6 D_{\mathrm{ps}} (R_{\mathrm{p}} + R_{\mathrm{s}})} \,. \tag{22.7}$$

The ratio of the two interaction energies, N, can be expressed as

$$N = \frac{W_{\mathrm{pw}}}{W_{\mathrm{ps}}} = \left(1 + \frac{R_{\mathrm{p}}}{R_{\mathrm{s}}}\right) \frac{A_{\mathrm{pw}} D_{\mathrm{ps}}}{A_{\mathrm{ps}} D_{\mathrm{pw}}} \,. \tag{22.8}$$

When the energy required to separate a particle from the wall is greater than that required to separate it from a spatula, self-cleaning will occur. For example, if

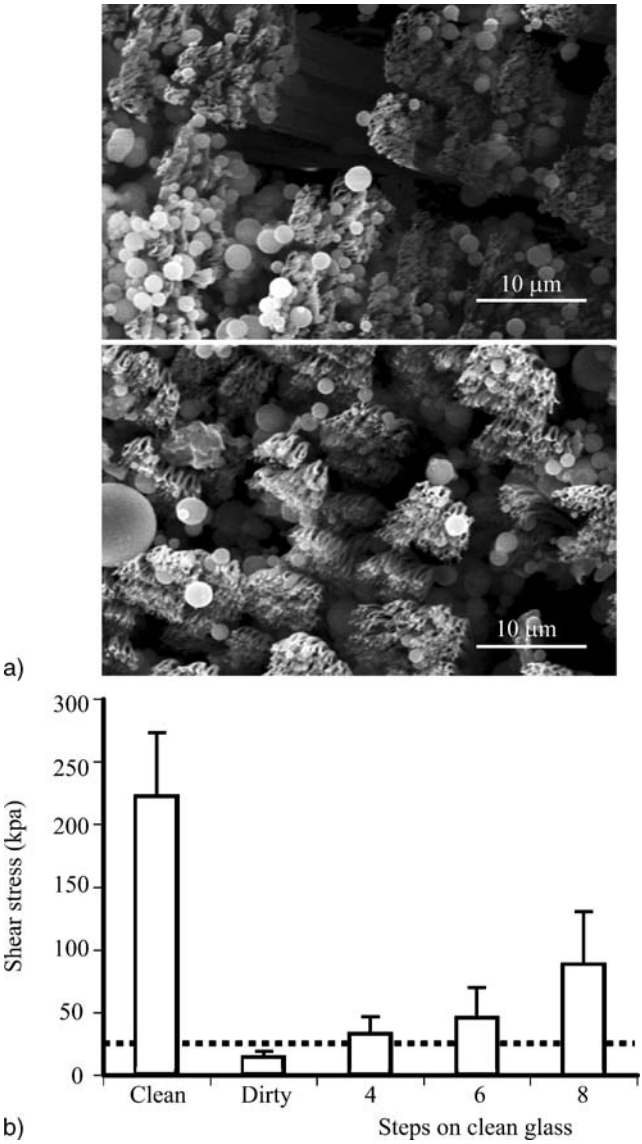

Fig. 22.6. (**a**) SEM images of spatulae after dirtying with microspheres (*top*) and after five simulated steps (*bottom*). (**b**) Mean shear stress exerted by a gecko on a surface after dirtying. The *dotted line* represents sufficient recovery to support body weight by a single toe [32]

$R_p = 2.5\,\mu m$ and $R_s = 0.1\,\mu m$ [59, 80], self-cleaning will occur as long as no more than 26 spatulae are attached to the dust particle at one time assuming similar Hamaker constants and gap distances. The maximum number of spatulae, as well as the percentage of available spatulae, in contact with a particle for self-cleaning to occur is tabulated in Table 22.2. It can be seen that very small particles (less than

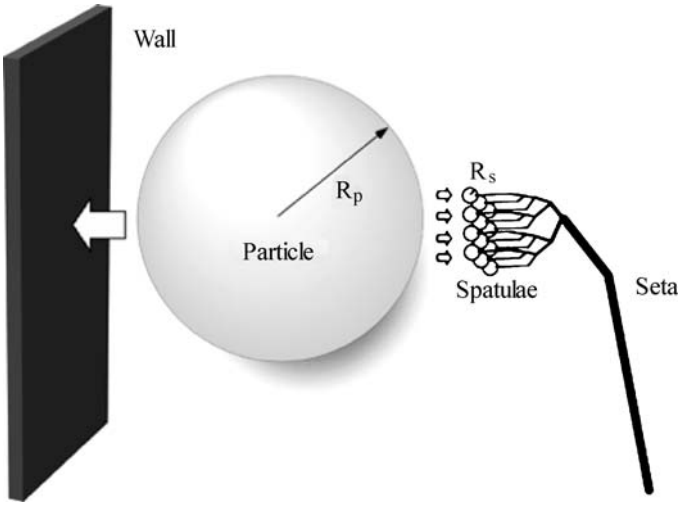

Fig. 22.7. Model of interactions between gecko spatulae of radius R_s, a spherical dirt particle of radius R_p, and a planar wall that enables self-cleaning [32]

Table 22.2. Maximum number of spatulae that can be in contact with a contaminant particle in order for self-cleaning to occur

Radius of particle (μm)	Maximum no. of spatulae in contact with particle	Area of sphere (μm^2)	Spatulae available	Percentage needed to adhere
0.1	2	0.03	0.25	804
0.5	6	0.79	6.2	96
1	11	3	25	44
2.5	26	19	156	17
5	51	79	622	8
10	101	314	2488	4
20	201	1257	9952	2

Spatula radius, R_s, is 0.1 μm

0.5-μm diameter) do not come into contact with enough spatulae to adhere. Owing to the curvature of larger particles relative to the planar field of the spatulae, very few spatulae are able to come into contact with the particle. As a result, Hansen and Autumn [32] concluded that self-cleaning should occur for all spherical spatulae interacting with all spherical particles.

22.3 Attachment Mechanisms

When asperities of two solid surfaces are brought into contact with each other, chemical and/or physical attractions occur. The force developed that holds the two

surfaces together is known as adhesion. In a broad sense, adhesion is considered to be either physical or chemical in nature [10–13, 16, 37, 43, 83]. Chemical interactions such as electrostatic attraction charges [64] as well as intermolecular forces [34] including van der Waals and capillary forces have all been proposed as potential adhesion mechanisms in gecko feet. Others have hypothesized that geckos adhere to surfaces through the secretion of sticky fluids [67, 78], suction [67], increased frictional force [36], and microinterlocking [19].

22.3.1 Unsupported Adhesive Mechanisms

Several of the aforementioned mechanisms have not been supported in testing. The rejected mechanisms of adhesion are summarized in Table 22.3.

Table 22.3. Proposed mechanisms of adhesion utilized by gecko feet and experimental evidence against and in favor of the proposed theories

Unsupported adhesive mechanisms			
Mechanism	Proposed by	Experimental evidence against	Disproven by
Secretion of sticky fluids	N/A	Geckos lack glands on their toes that produce sticky fluids capable of adhesion	[67, 78]
Suction	[67]	The adhesive force of a gecko is not affected in high-vacuum experiments	[19]
Electrostatic attraction	[64]	Geckos are able to adhere to surfaces in ionized air (which would eliminate electrostatic attraction)	[19]
Increased frictional force	[36]	Observations that a gecko can adhere upside down, even though frictional force only acts parallel to a surface	Numerous observers
Micro-interlocking	[19]	Measurements of large adhesive forces of a gecko seta on molecularly smooth SiO_2	[6]
Supported adhesive mechanisms			
Mechanism	Proposed by	Experimental evidence for	Supported by
Van der Waals forces (primary)	[34]	Overall and setal adhesion matches the theoretical adhesion values predicted by van der Waals forces	[6]
Capillary forces (secondary)	[34]	Adhesive force of a single gecko spatula was affected by relative humidity present in the air	[39]

22.3.1.1 Secretion of Sticky Fluids

Although several insects and frogs rely on sticky fluids to adhere to surfaces, geckos lack glands on their toes capable of producing these fluids [67, 78]. As a result, this hypothesis has been ruled out.

22.3.1.2 Suction

Simmermacher [67] proceeded to propose that geckos make use of miniature suction cups as an adhesive mechanism. Suction cups operate under the principle of microcapillary evacuation. When a suction cup comes into contact with a surface, air is forced out of the contact area, creating a pressure differential. The adhesive force generated is simply the pressure differential multiplied by the apparent area of contact [10].

Suction cups lose their adhesive strength when used under high-vacuum conditions since a pressure differential can no longer be developed. This mechanism of adhesion can be easily investigated by comparing adhesive force under a vacuum to adhesive force under atmospheric conditions. Experiments carried out in a vacuum by [19] did not show a difference between the adhesive force under these conditions compared with ambient conditions, thus rejecting suction as an adhesive mechanism.

22.3.1.3 Electrostatic Attraction

Electrostatic attraction occurs when two dissimilar heteropolar surfaces come in contact. Electrostatic forces are produced by one or more valence electrons transferring completely from one atom to another. When the separation between two surfaces is approximately equal to the atomic spacing (0.3 nm), the bond generated is quite strong and resembles that within the bulk material. If an insulator (e.g., gecko setae) is brought into contact with a metal, there is a large separation of charge at the interface that produces an electrostatic attraction [18, 20, 46, 72, 79]. Rubbing action during activities such as walking and running would increase the fraction of charged surface area. This is often referred to as the "triboelectric" effect [33, 66].

Schmidt [64] proposed electrostatic attraction as the mechanism of adhesion used by the gecko attachment system. Dellit [19] conducted experiments to determine the electrostatic contribution to gecko adhesion. This testing utilized X-ray bombardment to create ionized air and hence eliminate electrostatic attraction. It was determined that geckos were still able to adhere to surfaces in these conditions and, therefore, electrostatic charges could not be the sole cause of attraction.

22.3.1.4 Increased Frictional Force

It has also been postulated that the adhesive strength of gecko attachment pads arises from a large frictional force due to a large real area of contact [36]. The hierarchical

structure of lamellae–setae–branches–spatulae enables a gecko to create a real area of contact with a mating surface that is orders of magnitude greater than that with a nondivided surface. Since the coefficients of static and kinetic friction are dependent on contact area [12, 13], a large real area of contact would cause a large coefficient of friction. Under this theory, a gecko would be able to climb vertical walls if the frictional force exceeded the weight of the lizard. Although large frictional forces could enable geckos to walk up vertical surfaces, they would not account for a gecko's ability to cling to surfaces upside down. Frictional force only acts in the direction parallel to the contact surface, yet to hang upside down an adhesive force is required perpendicular to the surface. As a result, frictional force has been discounted as a potential mechanism.

22.3.1.5 Microinterlocking

Dellit [19] proposed that the curved shape of setae act as microhooks that catch on rough surfaces. This process known as microinterlocking would allow geckos to attach to rough surfaces. Autumn et al. [6] demonstrated the ability of a gecko to generate large adhesive forces when in contact with a molecularly smooth SiO_2 microelectromechanical system (MEMS) semiconductor. Since surface roughness is necessary for microinterlocking to occur, it has been ruled out as a mechanism of adhesion.

22.3.2 Supported Adhesive Mechanisms

Two mechanisms, van der Waals forces and capillary forces, remain as the potential sources of gecko adhesion. These attachment mechanisms are described in detail in the following sections and are summarized in Table 22.3.

22.3.2.1 Van der Waals Forces

Van der Waals bonds are secondary bonds that are weak in comparison with other physical bonds such as covalent, hydrogen, ionic, and metallic bonds. Unlike other physical bonds, van der Waals forces are always present regardless of separation and are effective from very large separations (approximately 50 nm) down to atomic separation (approximately 0.3 nm). The van der Waals force per unit area between two parallel surfaces, f_{vdW}, is given by [29, 42, 43]

$$f_{\mathrm{vdW}} = \frac{A}{6\pi D^3} \quad \text{for } D < 30\,\mathrm{nm}\,, \tag{22.9}$$

where A is the Hamaker constant and D is the separation between surfaces.

Hiller [34] showed experimentally that the surface energy of a substrate is responsable for Gecko adhesion. One potential adhesive mechanism would then be van der Waals forces [6, 73]. Assuming van der Waals forces to be the dominant adhesive mechanism utilized by geckos, we can calculate the adhesive force of a gecko.

Typical values of the Hamaker constant range from 4×10^{-20} to 4×10^{-19} J [43]. In the calculation, the Hamaker constant is assumed to be 10^{-19} J, the surface area of a spatula is taken to be 2×10^{-14} m^2 [5, 59, 80], and the separation between the spatula and the contact surface is estimated to be 0.6 nm. This equation yields the force of a single spatula to be about 0.5 μN. By applying the surface characteristics of Table 22.1, we find the maximum adhesive force of a gecko to be 150–1500 N for varying spatula density of 100–1000 spatulae per seta. If an average value of 550 spatulae per seta is used, the adhesive force of a single seta is approximately 270 μN, which is in agreement with the experimental value obtained by Autumn et al. [6], which will be discussed in Sect. 22.4.1.1.

Another approach to calculate adhesive force is to assume that spatulae are cylinders that terminate in hemispherical tips. By using (22.2) and assuming that the radius of each spatula is about 100 nm and that the surface energy is expected to be 50 mJ/m^2 [3], we can predict the adhesive force of a single spatula to be 0.02 μN. This result is an order of magnitude lower than the first approach calculated for the higher value of A. For a lower value of 10^{-20} J for the Hamaker constant, the adhesive force of a single spatula is comparable to that obtained using the surface-energy approach.

Several experimental results favor van der Waals forces as the dominant adhesive mechanism, including temperature testing [8] and adhesive-force measurements of a gecko seta with both hydrophilic and hydrophobic surfaces [6]. These data will be presented in Sects. 22.4.2–22.4.4.

22.3.2.2 Capillary Forces

It has been hypothesized that capillary forces that arise from liquid-mediated contact could be a contributing or even the dominant adhesive mechanism utilized by gecko spatulae [3, 73]. Experimental adhesion measurements (Sects. 22.4.3 and 22.4.4) conducted on surfaces with different hydrophobicities and at various humidities [39] support this hypothesis as a contributing mechanism. During contact, any liquid that wets or has a small contact angle on surfaces will condense from vapor in the form of an annular-shaped capillary condensate. Owing to the natural humidity present in the air, water vapor will condense to liquid on the surface of bulk materials. During contact this will cause the formation of adhesive bridges (menisci) owing to the proximity of the two surfaces and the affinity of the surfaces for condensing liquid [21, 58, 82].

Capillary forces can be divided into two components: a meniscus force from surface tension and a rate-dependent viscous force [11–13]. The total adhesive force is simply the sum of the two components. The meniscus contribution to adhesion between a spherical surface and a flat plate, F_{M}, is given by [50]

$$F_{\mathrm{M}} = 2\pi R\gamma_{\mathrm{l}} \left(\cos\theta_1 + \cos\theta_2\right) \ , \tag{22.10}$$

where R is the radius of the sphere, γ_{l} is the surface tension of the liquid, and θ_1 and θ_2 are the contact angles of the sphere and the plate, respectively. It should be noted that meniscus force is independent of film thickness. Consequently, even a film as

thin as a single monolayer can significantly influence the attraction between two surfaces [10–12, 43].

The viscous component of liquid-mediated adhesion is given by [50]

$$F_{\mathrm{v}} = \frac{\beta \eta_{\mathrm{l}}}{t_{\mathrm{s}}} \ , \tag{22.11}$$

where β is a proportionality constant, η_{l} is the dynamic viscosity of the liquid, and t_{s} is the time to separate the two surfaces. t_{s} is inversely related to the velocity of the interface during detachment. Furthermore, the fluid quantity has a weak dependence on viscous force.

22.4 Experimental Adhesion Test Techniques and Data

Experimental measurements of the adhesive force of a single gecko seta [6] and a single gecko spatula [38, 39] have been made. The effect of the environment, including temperature [8, 49] and humidity [39], has been studied. Some of the data have been used to understand the adhesive mechanism utilized by the gecko attachment system – van der Waals or capillary forces. The majority of experimental results point towards van der Waals forces as the dominant mechanism of adhesion [6, 8]. Recent research suggests that capillary forces can be a contributing adhesive factor [39].

22.4.1 Adhesion Under Ambient Conditions

Two feet of a Tokay gecko are capable of producing about 20 N of adhesive force with a pad area of about 220 mm^2 [41]. Under the assumption that there are 14,000 setae per square millimeter, the adhesive force from a single hair should be approximately 7 μN. It is likely that the magnitude is actually greater than this value because it is unlikely that all setae are in contact with the mating surface [6]. Setal orientation greatly influences adhesive strength. This dependency was first noted by Autumn et al. [6]. It was determined that the greatest adhesion occurs at 30°. In order to determine the adhesive mechanism(s) utilized by gecko feet, it is important to know the adhesive force of a single seta; hence, the adhesive force of gecko foot hair has been the focus of several investigations [6, 38].

22.4.1.1 Adhesive Force of a Single Seta

Autumn et al. [6] used both a MEMS force sensor and a wire as a force gauge to determine the adhesive force of a single seta. The MEMS force sensor is a dual-axis atomic force microscope (AFM) cantilever with independent piezoresistive sensors which allows simultaneous detection of vertical and lateral forces [17].

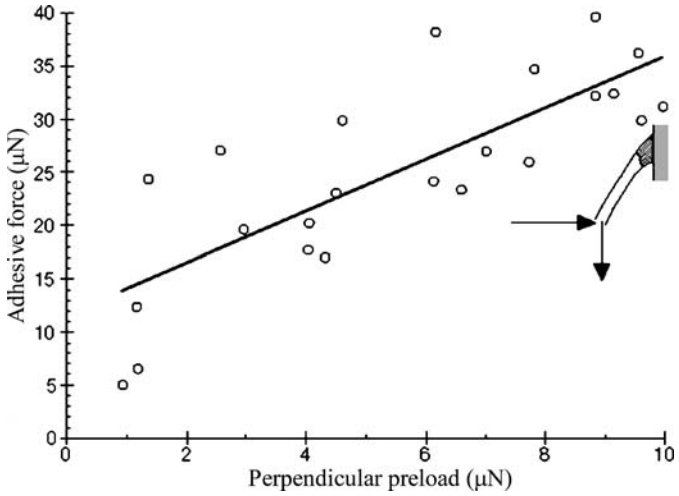

Fig. 22.8. Adhesive force of a single gecko seta as a function of applied preload. The seta was first pushed perpendicularly against the surface and then pulled parallel to the surface [6]

The wire force gage consisted of an aluminum bonding wire which displaced under a perpendicular pull. Autumn et al. [6] discovered that setal force actually depends on the three-dimensional orientation of the seta as well as on the preloading force applied during initial contact. Setae that were preloaded vertically to the surface exhibited only one tenth of the adhesive force ($0.6 \pm 0.7\ \mu N$) compared with setae that were pushed vertically and then pulled horizontally to the surface ($13.6 \pm 2.6\ \mu N$). The dependence of adhesive force of a single gecko spatula on the perpendicular preload is illustrated in Fig. 22.8. The adhesive force increases linearly with the preload, as expected [10–12]. The maximum adhesive force of a single gecko foot hair occurred when the seta was first subjected to a normal preload and then slid 5 μm along the contacting surface. Under these conditions, the adhesive force measured $194 \pm 25\ \mu N$ (approximately 10 atm adhesive pressure).

22.4.1.2 Adhesive Force of a Single Spatula

Huber et al. [38] used atomic force microscopy to determine the adhesive force of individual gecko spatulae. A seta with four spatulae was glued to an AFM tip. The seta was then brought into contact with a surface and a compressive preload of 90 nN was applied. The force required to pull the seta off of the surface was then measured. As seen in Fig. 22.9, there are two distinct peaks on the graph – one at 10 nN and the other at 20 nN. The first peak corresponds to one of the four spatulae adhering to the contact surface, while the peak at 20 nN corresponds to two of the four spatulae adhering to the contact surface. The average adhesive force of a single spatula was found to be 10.8 ± 1 nN. The measured value is in agreement with the measured adhesive strength of an entire gecko (on the order of 10^9 spatulae on a gecko).

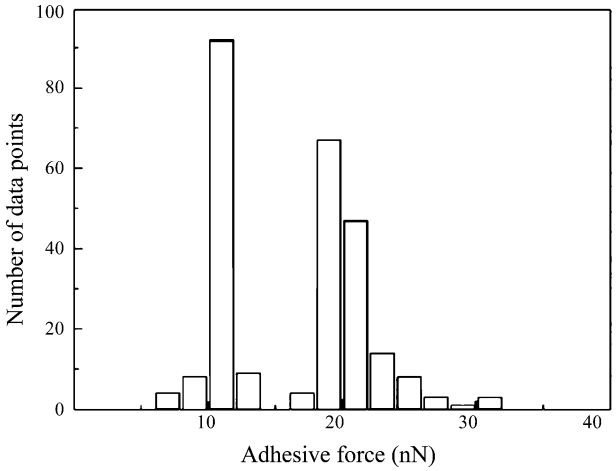

Fig. 22.9. Adhesive force of a single gecko spatula. The peak at 10 nN corresponds to the adhesive force of one spatula and the peak at 20 nN corresponds to the adhesive force of two spatulae [39]

22.4.2 Effects of Temperature

Environmental factors are known to affect several aspects of vertebrate function, including speed of locomotion, digestion rate, and muscle contraction, and as a result several studies have been completed to investigate environmental impact on these functions. Relationships between the environment and other properties such as adhesion have been far less studied [8]. Only two known studies exist that examine the effect of temperature on the clinging force of the gecko [8, 49]. Losos [49] examined adhesive ability of large live geckos at temperatures up to 17 °C. Bergmann and Irschick [8] expanded upon this research for body temperatures ranging from 15 to 35 °C. The geckos were incubated until their body temperature reached the desired level. The clinging ability of these animals was then determined by measuring the maximum force exerted by the geckos as they were pulled off a custom-built force plate. The clinging force of a gecko for the experimental test range is plotted in Fig. 22.10. It was determined that variation in temperature is not statistically significant for the adhesive force of a gecko. From these results, it was concluded that the temperature independence of adhesion supports the hypothesis of clinging as a passive mechanism (i.e., van der Waals forces). Both studies only measured overall clinging ability on the macroscale. There have not been any investigations into the effects of temperature on the clinging ability of a single seta on the microscale and therefore testing in this area is extremely important.

22.4.3 Effects of Humidity

Huber et al. [39] employed similar methods to Huber et al. [38] (discussed in Sect. 22.4.1.2) in order to determine the adhesive force of a single spatula at varying humidity. Measurements were made using an AFM placed in an air-tight chamber.

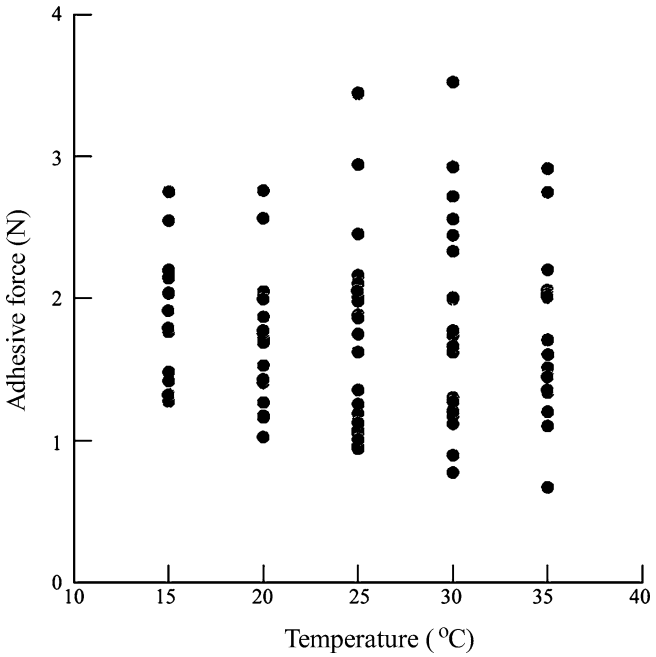

Fig. 22.10. Adhesive force of a gecko as a function of temperature [8]

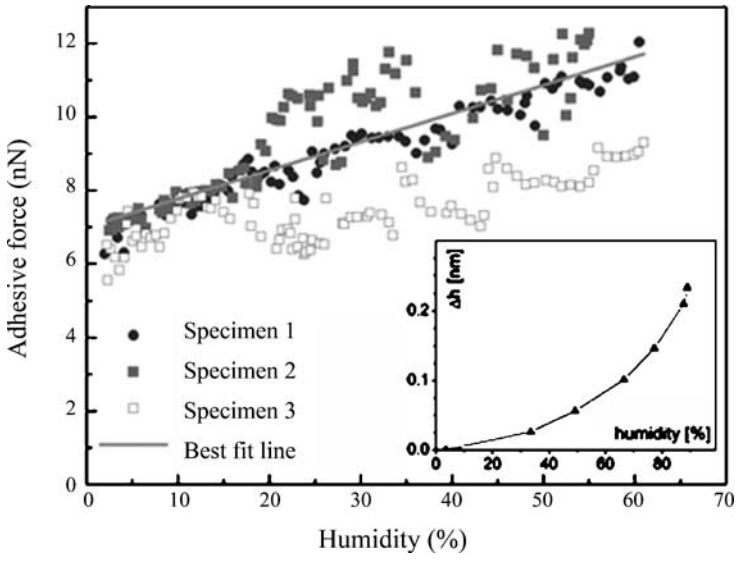

Fig. 22.11. Humidity effects on spatular pull-off force. *Inset*: The increase in water film thickness on a Si wafer with increasing humidity [39]

The humidity was adjusted by varying the flow rate of dry nitrogen into the chamber. The air was continuously monitored with a commercially available hygrometer. All tests were conducted at ambient temperature.

As seen in Fig. 22.11, even at low humidity, the adhesive force is large. An increase in humidity further increases the overall adhesive force of a gecko spatula. The pull-off force roughly doubled as the humidity was increased from 1.5 to 60%. This humidity effect can be explained in two possible ways: (1) by standard capillarity or (2) by a change of the effective short-range interaction due to absorbed monolayers of water – in other words, the water molecules increase the number of van der Waals bonds that are made. On the basis of these data, van der Waals forces are the primary adhesive mechanism and capillary forces are a secondary adhesive mechanism.

22.4.4 Effects of Hydrophobicity

To further test the hypothesis that capillary forces play a role in gecko adhesion, the spatular pull-off force was determined for contact with both hydrophilic and hydrophobic surfaces. As seen in Fig. 22.12a, the capillary adhesion theory predicts that a gecko spatula will generate a greater adhesive force when in contact with a hydrophilic surface compared with a hydrophobic surface, while the van der Waals adhesion theory predicts that the adhesive force between a gecko spatula and a surface will be the same regardless of the hydrophobicity of the surface [7]. Figure 22.12b shows the adhesive pressure of a whole gecko and the adhesive force of a single seta on hydrophilic and hydrophobic surfaces. The data show that the adhesive values are the same on both surfaces. This supports the van der Waals prediction of Fig. 22.12a. Huber et al. [39] found that the hydrophobicity of the attachment surface had an effect on the adhesive force of a single gecko spatula as shown in Fig. 22.12c. These results show that adhesive force has a finite value for superhydrophobic surface and increases as the surface becomes hydrophilic. It is concluded that van der Waals forces are the primary mechanism and capillary forces further increase the adhesive force generated.

22.5 Design of Biomimetic Fibrillar Structures

22.5.1 Verification of Adhesion Enhancement of Fabricated Surfaces Using Fibrillar Structures

In order to create a material capable of dry adhesion, one would want to mimic the hierarchical structures found on the attachment pads of insects and lizards. Peressadko and Gorb [55] investigated whether adhesion enhancement was experienced through a division of contact area or fibrillar structure. The adhesive strength of a patterned surface and a smooth surface (roughness amplitude, $R_a = 0.5$ nm) of poly(vinyl siloxane) (PVS) was tested on both a smooth and a curved glass surface.

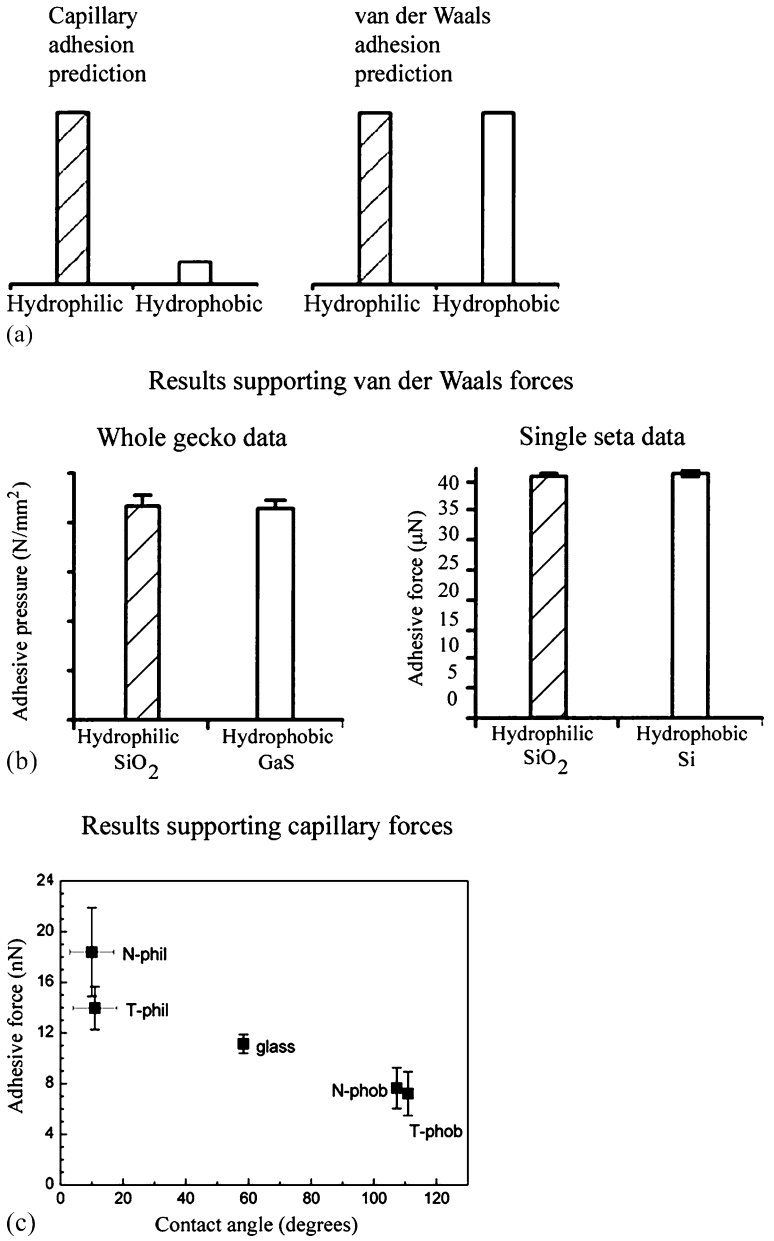

Fig. 22.12. (**a**) Capillary and van der Waals adhesion predictions for the relative magnitude of the adhesive force of gecko setae with hydrophilic and hydrophobic surfaces [7]. (**b**) Results of adhesion testing for a whole gecko and a single seta with hydrophilic and hydrophobic surfaces [7]. (**c**) Results of adhesive force testing with surfaces with different contact angles [39]

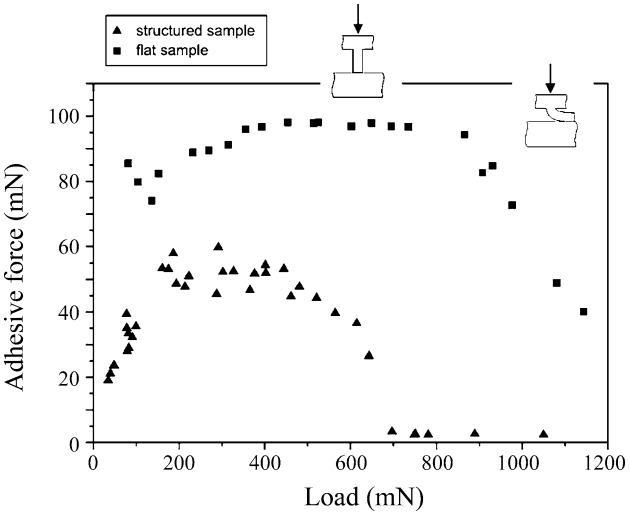

Fig. 22.13. Adhesive force of structured and flat poly(vinyl siloxane) samples with a flat glass surface [55]

Both PVS surfaces were molded. The patterned surface consisted of 72 columns (height 400 μm, cross section 250 μm × 125 μm). The samples were loaded perpendicular to the glass surface. During unloading, the adhesive force was measured. As seen in Fig. 22.13, the adhesive strength of the structured sample was several times greater than that of the flat sample. The adhesive strength of the fibrillar sample decreases at a load beyond 800 mN. This decline in adhesion is due to column buckling. Although the testing only dealt with surfaces made of PVS, one can assume that similar adhesion enhancement would result in structured samples of any material.

22.5.2 Contact Mechanics of Fibrillar Structures

In order for a fibrillar microstructure to act as a good adhesive, it is necessary that the materials be compliant. This allows the fibrillar interface to make contact at as many points as possible. The mechanics of adhesion between a fibrillar structure and a rough surface have been a topic of investigation for many researchers [24, 27, 28, 45, 56, 70]. In order to better understand the mechanics of adhesion, the approach of [45] will be described. The fibrillar surface is modeled in two dimensions, as shown in Fig. 22.14a, and is described by the length, L, and width, $2a$, of the fibrils, and by the area fraction of the interface covered by fibril ends, f. Fibrils composed of two different materials are investigated, a soft material and a hard material. Both of these materials are assumed to be linear-elastic and have properties corresponding to those given in Table 22.4.

If one wants to achieve the intimate contact between an elastic solid and a wavy surface given by (22.4), a compressive stress, S_c, must be applied to the surface. Intimate contact is achieved when [40]

$$\frac{\pi E h}{2(1-\nu^2)S_c\lambda} < 1 \,, \tag{22.12}$$

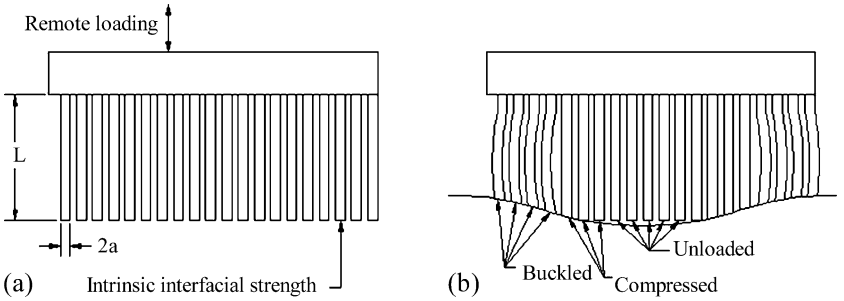

Fig. 22.14. Geometry of (**a**) a model fibrillar structure and (**b**) a fibrillar mat loaded in compression against a rough surface

Table 22.4. Material properties for a soft, good adhesive and a stiff, weak adhesive [45]

Parameter	Soft, good adhesive	Stiff, weak adhesive
Young's modulus, E (Pa)	10^6	10^9
Interfacial fracture energy, Γ_0 (J/m^2)	100	1
Interfacial strength, σ^* (Pa)	10^6	10^3
Applied stress, σ (Pa)	10^4	10^4

where E is Young's modulus and ν is Poisson's ratio. By substituting the values of Table 22.4 into this equation, we can see that soft and hard materials can tolerate surface roughness aspect ratios, h/λ, of approximately 5×10^{-3} and 5×10^{-6}, respectively.

If the fibrillar surface is to make contact with a rough surface, the fibrillar mat will be loaded as seen in Fig. 22.14b. The buckling stress, S_b, is given by [75]

$$\frac{S_\mathrm{b}}{E} = \frac{1}{3} f\pi^2 \left(\frac{a}{L}\right)^2 . \tag{22.13}$$

If f is taken to be 0.75, the width-to-length ratio, a/L, must be less than or equal to 0.064 for the soft material and 0.002 for the hard material in order for uniform contact to occur.

When long, slender beams (such as setae or nanobumps) are in close proximity, the potential for two adjacent members to adhere laterally to each other arises as depicted in Fig. 22.15. Hui et al. [40] determined a relation to check for this phenomenon:

$$\frac{L}{2a}\left(\frac{2\gamma_\mathrm{s}}{3Ea}\right)^{1/4} < \left(\frac{w}{a}\right)^{1/2} , \tag{22.14}$$

where w is the gap between fibrils and γ_s is the surface energy (0.05 J/m^2). Under the assumption that $w/a = 1$, the width-to-length ratio must be greater than or equal to 0.25 and 0.045 for the soft and hard materials, respectively.

It is evident when comparing the results of (22.13) and (22.14) that it is not possible for all of the fibrils to be in contact with the sinusoidal surface of (22.4). As a result, there is a trade-off between the aspect ratio of the fibrils and their adaptability

to a rough surface. If the aspect ratio of the fibrils is too large, they can adhere to each other or even collapse under their own weight, as shown in Fig. 22.16a. If the aspect ratio is too small (Fig. 22.16b), the structures will lack the necessary compliance to conform to a rough surface.

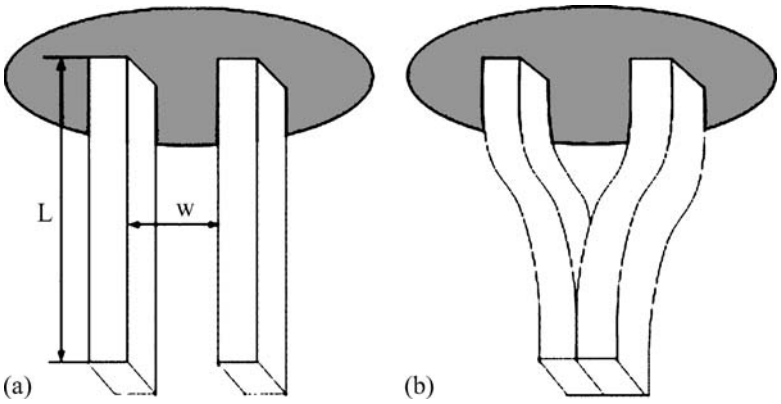

Fig. 22.15. Model of two adjacent fibers adhering laterally to each other [24]

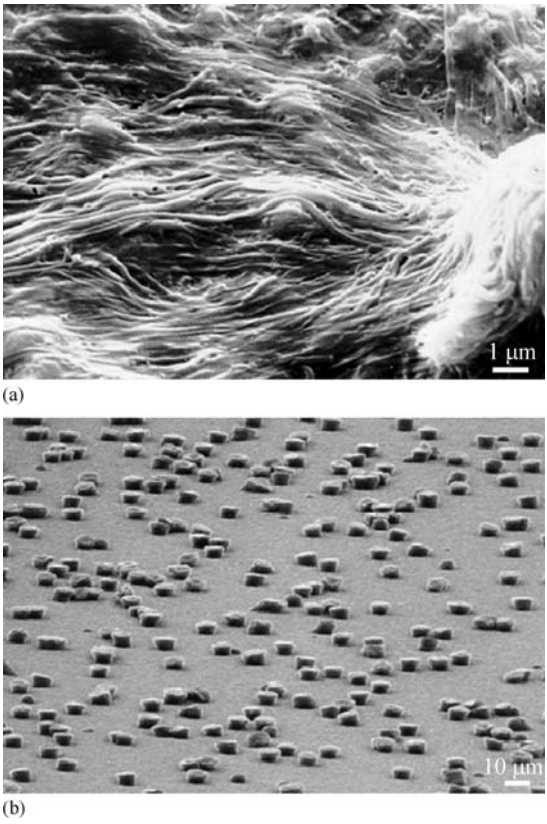

Fig. 22.16. SEM micrographs of (**a**) high aspect ratio polymer fibrils that have collapsed under their own weight and (**b**) low aspect ratio polymer fibrils that are incapable of adapting to rough surfaces [69]

22.5.3 Fabrication of Biomimetric Gecko Skin

On the basis of studies found in the literature, the dominant adhesive mechanism utilized by geckos and other spider-attachment systems appears to be van der Waals forces. The complex divisions of the gecko skin (lamellae–setae–branches–spatulae) enable a large real area of contact between the gecko skin and mating surface. Hence, a hierarchical fibrillar microstructure/nanostructure is desirable for dry, superadhesive tapes [45]. The development of a nanocomposite capable of replicating this adhesive force developed in nature is limited by current fabrication techniques.

On the microscale/nanoscale, typical machining methods (e.g., forging, drilling, grinding, lapping) are not possible. In order to create nanobumps, other manufacturing techniques are required and have been the subject of numerous studies [25, 52, 53, 68, 70, 71, 81].

22.5.3.1 Single-Level Hierarchical Structures

Previously, AFM tips were used to create a set of dimples on a wax surface in a process like that depicted in Fig. 22.17. These dimples served as a mold for creating polymer nanopyramids [70]. The adhesive force to an individual pyramid was measured using another AFM cantilever. The force was found to be about 200 μN. Although each pyramid of the material is capable of producing similar forces to that of a gecko seta, it failed to replicate adhesion on a large scale. This was due to the lack of flexibility in the pyramids. In order to ensure that the largest possible area of contact occurs between the tape and mating surface, a soft, compliant fibrillar structure is desired [45]. As shown in previous calculations, the van der Waals adhesive force for two parallel surfaces is inversely proportional to the cube of the distance between two surfaces.

Geim et al. [25] created arrays of nanohairs using electron-beam lithography and dry etching in oxygen plasma (Fig. 22.18a). The original arrays were created on a rigid silicon wafer. This design was only capable of creating 0.01 N of adhesive force for a 1-cm^2 patch. The nanohairs were then transferred from the silicon wafer to a soft bonding substrate. A 1-cm^2 sample was able to create 3 N of adhesive force under the new arrangement. This is approximately one third the adhesive strength of a gecko. Bunching (as described earlier) was determined to greatly reduce the durability and adhesive strength of the polymer tape. The bunching can be clearly seen in Fig. 22.18b.

Multiwalled carbon nanotube (MWCNT) hairs have been used to create superadhesive tapes [81]. The first step in the creation of this surface involves the growth of 50–100 μm MWCNTs on quartz or silicon substrates through chemical vapor deposition. Patterns are then created using a combination of photolithography and a wet and/or dry etching. SEM images of the nanotube surfaces can be seen in Fig. 22.19. On a small scale (nanometer level), the MWCNT surface was able to achieve adhesive forces 200 times greater than those of gecko foot hairs. However, the MWCNT surface could not replicate large scale gecko adhesion due to a lack of compliance.

Directed self-assembly could be used to produce regularly spaced fibers [62, 68]. In this technique, a thin liquid polymer film is coated on a flat conductive substrate.

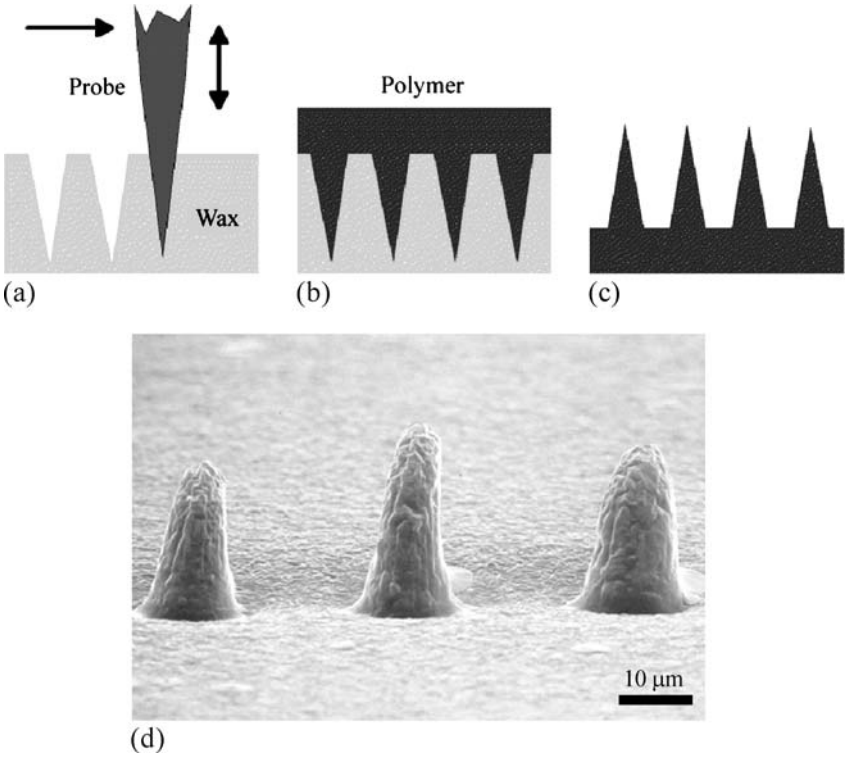

Fig. 22.17. (**a**) Indenting a flat wax surface using a sharp probe (nanotip indenting), (**b**) molding with a polymer, and (**c**) separating the polymer from the wax surface by peeling. (**d**) SEM image of three pillars created by nanotip indentation [68]

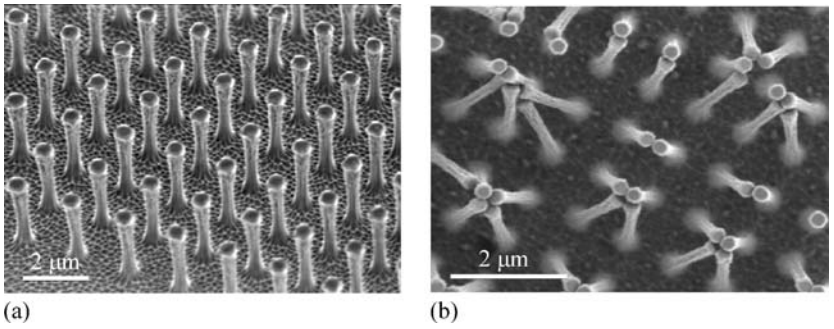

Fig. 22.18. SEM images of (**a**) an array of polyimide nanohairs and (**b**) bunching of the nanohairs, which leads to a reduction in adhesive force [25]

As demonstrated in Fig. 22.20, a closely spaced metal plate is used to apply a direct current electric field on the polymer film. Owing to instabilities, pillars will begin to grow. Self-assembly is desirable because the components spontaneously assemble, typically by bouncing around in a solution or gas phase until a stable structure of

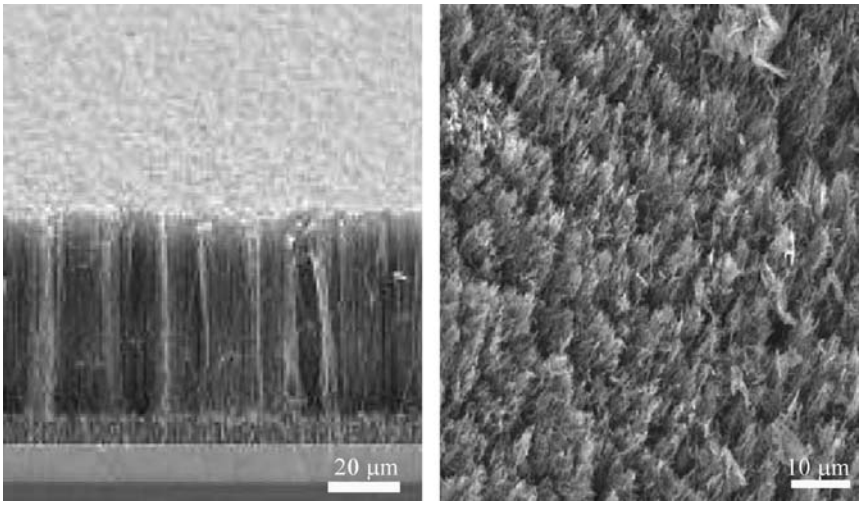

Fig. 22.19. SEM images of multiwalled carbon nanotube structures: *left* grown on silicon by vapor deposition and *right* transferred into a poly(methyl methacrylate) matrix and then exposed on the surface after solvent etching [81]

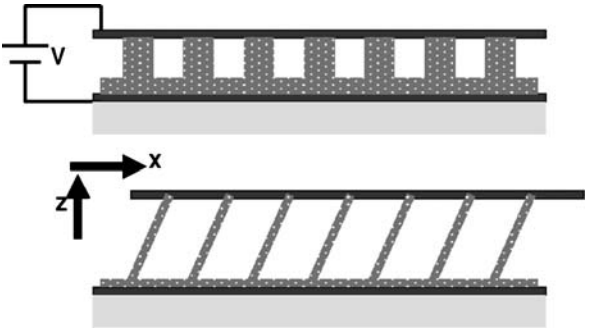

Fig. 22.20. Directed self-assembly-based method of producing high aspect ratio microhairs/nanohairs [68]

minimum energy is reached. This method is crucial in biomolecular nanotechnology, and has the potential to be used in precise devices [1]. These surface coatings have been demonstrated to be both durable and capable of creating superhydrophobic conditions and have been used to form clusters on the nanoscale [54].

22.5.3.2 Multilevel Hierarchical Structures

The aforementioned fabricated surfaces only have one level of hierarchy. Although these surfaces are capable of producing high adhesion on the microscale/nanoscale, all have failed in producing large-scale adhesion owing to a lack of compliance and bunching. In order to overcome these problems, Northen and Turner [52, 53] created a multilevel compliant system by employing a microelectromechanical-based approach. They created a layer of nanorods which they deemed "organorods"

(Fig. 22.21a). These organorods are comparable in size to that of gecko spatulae (50–200 nm in diameter and 2-μm tall). They sit atop a silicon dioxide chip (approximately 2-μm thick and 100–150 μm across a side), which was created using photolithography (Fig. 22.21b). Each chip is supported on top of a pillar (1 μm in diameter and 50 μm tall) that attaches to a silicon wafer (Fig. 22.21c). The multilevel structures have been created across a 100-mm wafer (Fig. 22.21d).

Adhesion testing was performed using a nanorod surface on a solid substrate and on the multilevel structures. As seen in Fig. 22.22, adhesive pressure of the multilevel structures was several times higher than that of the surfaces with only one level of hierarchy. The durability of the multilevel structure was also much greater than that of the single-level structure. The adhesion of the multilevel structure did not change between iterations one and five. During the same number of iterations, the adhesive pressure of the single-level structure decreased to zero.

Sitti [68] proposed a nanomolding technique for creating structures with two levels of hierarchy. In this method, two different molds are created – one with pores on the order of microns in diameter and a second with pores of nanometer-scale diameter. As seen in Fig. 22.23, the two molds would be bonded to each other and then filled with a liquid polymer. According to [68], the method would enable the manufacturing of a high volume of synthetic gecko foot hairs at low cost.

The literature clearly indicates that in order to create a dry superadhesive, a fibrillar surface construction is necessary to maximize the van der Waals forces by decreasing the distance between the two surfaces. It is also desirable to have a su-

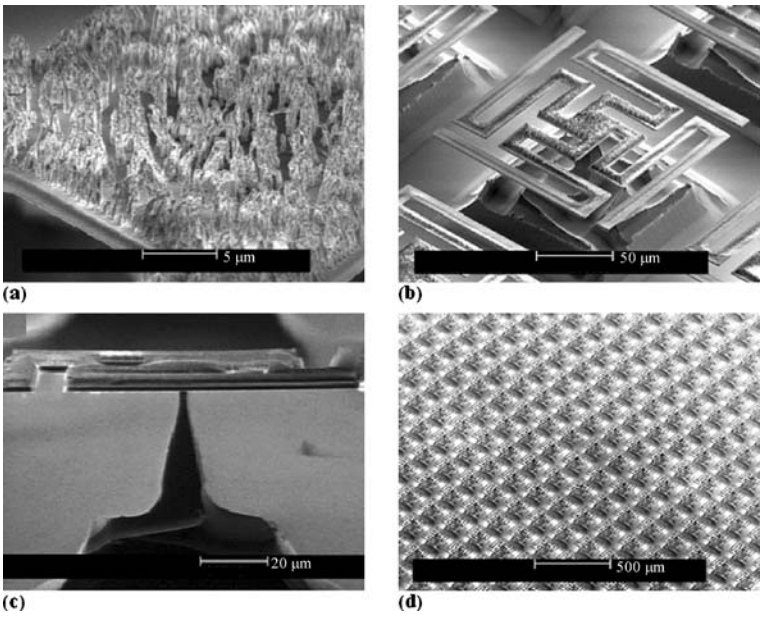

Fig. 22.21. Multilevel fabricated adhesive structure composed of (**a**) organorods, (**b**) silicon dioxide chips, and (**c**) support pillars. (**d**) This structure was repeated multiple times over a silicon wafer [52, 53]

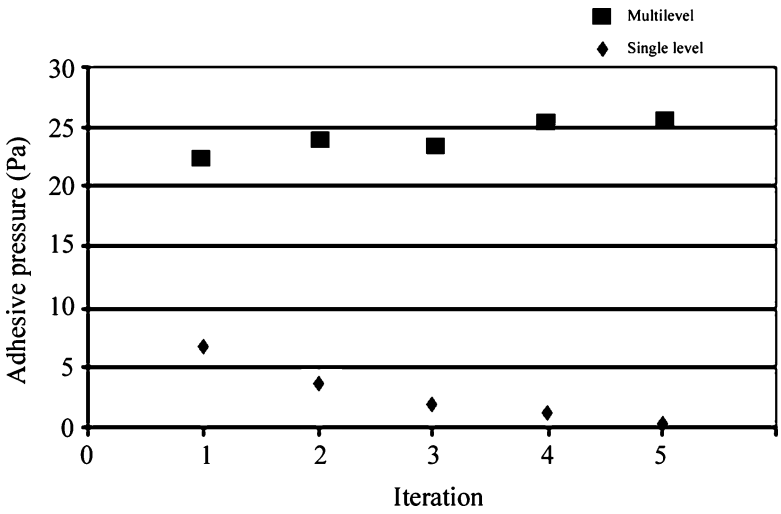

Fig. 22.22. Adhesion test results of a multilevel hierarchical structure (*top*) and a single-level hierarchical structure (*bottom*) repeated for five iterations [53]

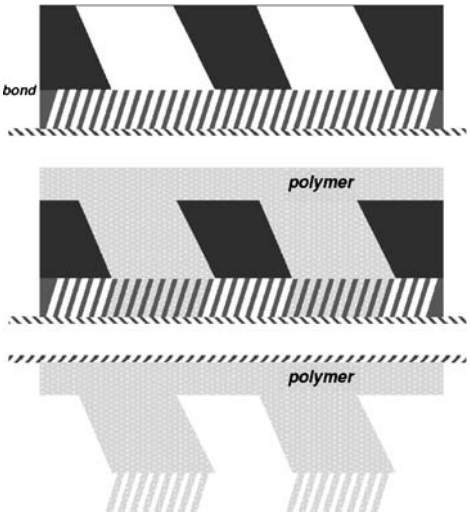

Fig. 22.23. Proposed process of creating multilevel synthetic gecko foot hairs using nanomolding. Micron- and nanometer-sized pore membranes are bonded together (*top*) and filled with liquid polymer (*middle*). The membranes are then etched away leaving the polymer surface (*bottom*) [68]

perhydrophobic surface in order to utilize self-cleaning. The material must be soft enough to conform to rough surfaces yet hard enough to avoid bunching, which will decrease the adhesive force.

22.6 Closure

The adhesive properties of geckos and other creatures, such as flies, beetles, and spiders, are due to the hierarchical structures present on each creature's attachment

pads. Geckos have developed the most intricate adhesive structures of any of the aforementioned creatures. The attachment system consists of ridges called lamellae that are covered in microscale setae that branch off into nanoscale spatulae. Each structure plays an important role in adapting to surface roughness, bringing the spatulae in close proximity with the mating surface. These structures as well as material properties allow the gecko to obtain a much larger real area of contact between its feet and a mating surface than is possible with a nonfibrillar material. Two feet of a Tokay gecko have about 220 mm^2 of attachment pad area on which the gecko is able to generate approximately 20 N of adhesive force. Although capable of generating high adhesive forces, a gecko is able to detach from a surface at will – an ability known as reversible adhesion or smart adhesion. Detachment is achieved by a peeling motion of the gecko's feet from a surface.

Van der Waals forces are widely accepted in the literature as the dominant adhesive mechanism utilized by hierarchical attachment systems. Capillary forces created by humidity naturally present in the air can further increase the adhesive force generated by the spatulae. Experimental results have supported the adhesive theories of intermolecular forces (van der Waals) as a primary adhesive mechanism and capillary forces as a secondary mechanism, and have been used to rule out several other mechanisms of adhesion, including the secretion of sticky fluids, suction, and increased frictional forces. Atomic force microscopy has been employed by several investigators to determine the adhesive strength of gecko foot hairs. The measured values of the maximum adhesive force of a single seta (194 μN) and of a single spatula (11 nN) are comparable to the van der Waals prediction of 270 μN and 11 nN for a seta and a spatula, respectively. The adhesive force generated by a seta increases with preload and reaches a maximum when both perpendicular and parallel preloads are applied. Although gecko feet are strong adhesives, they remain free of contaminant particles through self-cleaning. Spatular size along with material properties enable geckos to easily expel any dust particles that come into contact with their feet.

There is great interest among the scientific community to create surfaces that replicate the adhesive strength of gecko feet. These surfaces would be capable of reusable dry adhesion and would have uses in a wide range of applications from everyday objects such as tape, fasteners, and toys to microelectric and space applications and even wall-climbing robots. In the design of fibrillar structures, it is necessary to ensure that the fibrils are compliant enough to easily deform to the mating surface's roughness profile, yet rigid enough to not collapse under their own weight. Spacing of the individual fibrils is also important. If the spacing is too small, adjacent fibrils can attract each other through intermolecular forces, which will lead to bunching.

Nanoindentation, electron-beam lithography, and growing of carbon nanotube arrays are all methods that have been used to create fibrillar structures. The limitations of current machining methods on the microscale/nanoscale have resulted in the majority of fabricated surfaces consisting of only one level of hierarchy. Although typically capable of producing a large adhesive force with an individual fibril, all of these surfaces have failed to generate large adhesive forces on the macroscale. Bunching, lack of compliance, and lack of durability are all problems that have arisen with the aforementioned structures. Recently, a multilayered compliant system was cre-

ated using a microelectromechanical-based approach in combination with nanorods. This method as well as other proposed methods of multilevel nanomolding and directed self-assembly show great promise in the creation of adhesive structures with multiple levels of hierarchy, much like those of gecko feet.

Appendix

Several natural (sycamore tree bark and siltstone) and artificial (dry wall, wood laminate, steel, aluminum, and glass) surfaces were chosen to determine the microscale surface parameters of typical rough surfaces that a gecko might encounter. An Alpha-step 200 stylus profiler (Tencor Instruments, Mountain View, CA, USA) was used to obtain surface profiles of three different length scales: 80 μm, which is

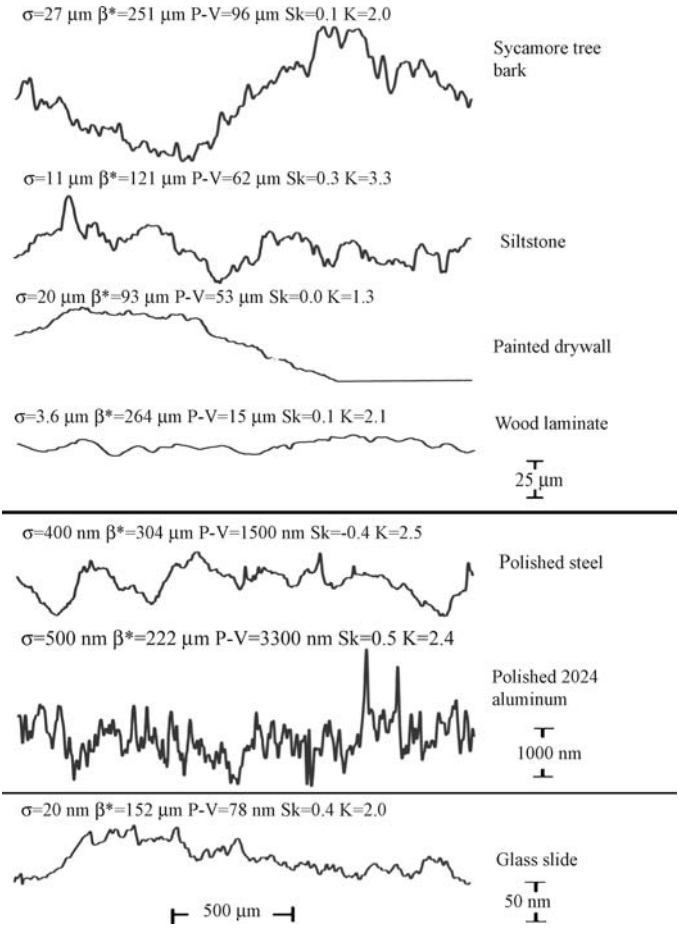

Fig. 22.24. (**a**) Surface height profiles of various random rough surfaces of interest at a 2000-μm scan length and (**b**) a comparison of the profiles of two surfaces at 80, 400, and 2000-μm scan lengths [15]

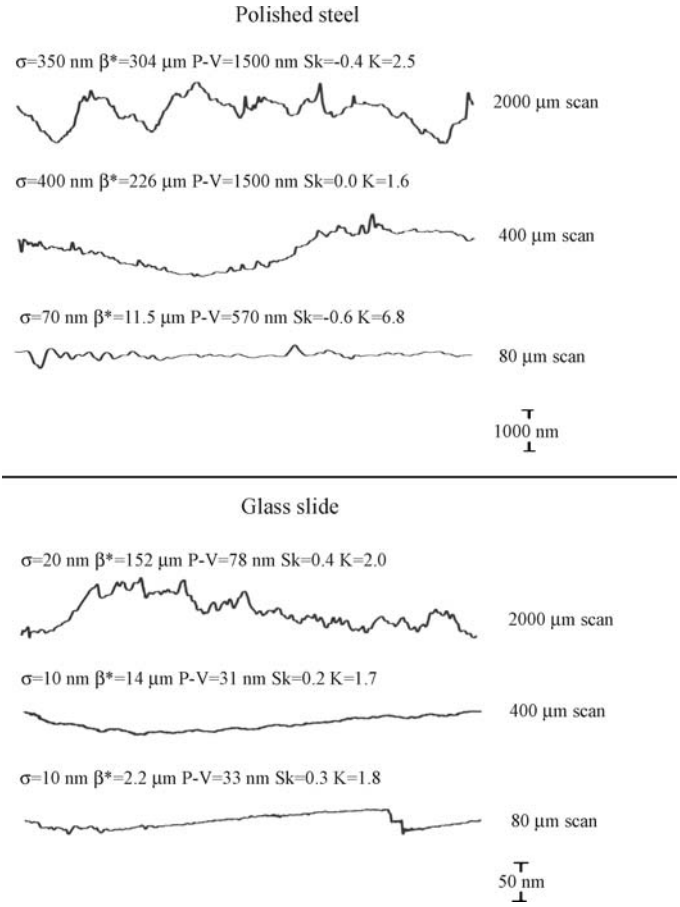

Fig. 22.24. (continued)

approximately the size of a single gecko seta; 2000 μm, which is close to the size of a gecko lamella; and an intermediate scan length of 400 μm. The radius of the stylus tip was 1.5–2.5 μm and the applied normal load was 30 μN (3 mg). The surface profiles were then analyzed using a specialized computer program to determine the root-mean-square amplitude, σ, correlation length, β^*, peak-to-valley distance, P–V, skewness, Sk, and kurtosis, K.

Samples of surface profiles and their corresponding parameters at a scan length of 2000 μm can be seen in Fig. 22.24a. The roughness amplitude, σ, varies from as low as 0.01 μm in glass to as high as 30 μm in tree bark. Similarly, the correlation length varies from 2 to 300 μm. The scale dependency of the surface parameters is illustrated in Fig. 22.24b. As the scan length of the profile increases, so too does the roughness amplitude and correlation length. Table 22.5 summarizes the scale-dependent factors σ and β^* for all seven sampled surfaces. At a scale length of 80 μm (size of seta), the roughness amplitude does not exceed 5 μm, while at a scale

Table 22.5. Scale dependence of surface parameters σ and β^* for rough surfaces at scan lengths of 80 and 2000 μm

Surface	Scan length 80 μm		2000 μm	
	σ (μm)	β^* (μm)	σ (μm)	β^* (μm)
Sycamore tree bark	4.4	17	27	251
Silitstone	1.1	4.8	11	268
Painted drywall	1	11	20	93
Wood laminate	0.11	18	3.6	264
Polished steel	0.07	12	0.40	304
Polished 2024 aluminum	0.40	6.5	0.50	222
Glass	0.01	2.2	0.02	152

length of 2000 μm (size of lamella), the roughness amplitude is as high as 30 μm. This suggests that setae are responsible for adapting to surfaces with roughness on the order of several micrometers, while lamellae must adapt to roughness on the order of tens of micrometers. Greater roughness values would be adapted to by the skin of the gecko. The spring model of Bhushan et al. [15] verifies that setae are only capable of adapting to roughness of a few microns and suggests that lamellae are responsible for adaptation to rougher surfaces.

References

1. Anonymous (2002) Self-assembly, Merriam-Webster's Medical Dictionary, Merriam-Webster, New York
2. Aristotle (1918) Historia Animalium. Book IX, Part 9, translated by Thompson DAW http://classics.mit.edu/Aristotle/history_anim.html
3. Arzt E, Gorb S, Spolenak R (2003) From micro to nano contacts in biological attachment devices. Proc Natl Acad Sci USA 100:10603–10606
4. Autumn K (2006) How gecko toes stick. Am Sci 94:124–132
5. Autumn K, Peattie AM (2002) Mechanisms of adhesion in geckos. Integr Comp Biol 42:1081–1090
6. Autumn K, Liang YA, Hsieh ST, Zesch W, Chan WP, Kenny TW, Fearing R, Full RJ (2000) Adhesive force of a single gecko foot-hair. Nature 405:681–685
7. Autumn K, Sitti M, Liang YA, Peattie AM, Hansen WR, Sponberg S, Kenny TW, Fearing R, Israelachvili JN, Full RJ (2002) Evidence for van der Waals adhesion in gecko setae. Proc Natl Acad Sci USA 99:12252–12256
8. Bergmann PJ, Irschick DJ (2005) Effects of temperature on maximum clinging ability in a diurnal gecko: evidence for a passive clinging mechanism? J Exp Zool 303A:785–791
9. Bertram JEA, Gosline JM (1987) Functional design of horse hoof keratin: the modulation of mechanical properties through hydration effects. J Exp Biol 130:121–136
10. Bhushan B (1996) Tribology and Mechanics of Magnetic Storage Devices. 2nd edn, Springer, Berlin, Heidelberg, New York
11. Bhushan B (1999) Principles and Applications of Tribology, Wiley, New York
12. Bhushan B (2002) Introduction to Tribology, Wiley, New York
13. Bhushan B (2005) Introduction to Nanotribology and Nanomechanics. Springer, Berlin, Heidelberg, New York

14. Bhushan B (2006) Springer Handbook of Nanotechnology. 2nd edn, Springer, Berlin, Heidelberg, New York
15. Bhushan B, Peressadko AG, Kim TW (2006) Adhesion analysis of two-level hierarchical morphology in natural attachment systems for smart adhesion. J Adhesion Sci Technol (in press)
16. Bikerman JJ (1961) The Science of Adhesive Joints, Academic, New York
17. Chui BW, Kenny TW, Mamin HJ, Terris BD, Rugar D (1998) Independent detection of vertical and lateral forces with a sidewall-implanted dual-axis piezoresistive cantilever. Appl Phys Lett 72:1388–1390
18. Davies DK (1973) Surface charge and the contact of elastic solids, J Phys D Appl Phys 6:1017–1024
19. Dellit WD (1934) Zur Anatomie und Physiologie der Geckozehe, Jena. Z Naturwiss 68:613–658
20. Derjaguin BV, Krotova NA, Smilga VP (1978) Effect of contact deformations on the adhesion of particles. J Colloid Interface Sci 53:314–326
21. Fan PL, O'Brien MJ (1975) Adhesion in deformable isolated capillaries. In: Lee LH (ed) Adhesion Science and Technology, Vol 9A, Plenum, New York, p 635
22. Federle W, Riehle M, Curtis ASG, Full RJ (2002) An integrative study of insect adhesion: mechanics of wet adhesion of pretarsal pads in ants. Integr Comp Biol 42:1100–1106
23. Full RJ, Fearing RS, Kenny TW, Autumn K (2004) Adhesive microstructure and method of forming same. US Patent 6,737,160
24. Gao H, Wang X, Yao H, Gorb S, Arzt E (2005) Mechanics of hierarchical adhesion structures of geckos. Mech Mater 37:275–285
25. Geim AK, Dubonos SV, Grigorieva IV, Novoselov KS, Zhukov AA, Shapoval SY (2003) Microfabricated adhesive mimicking gecko foot-hair. Nat Mater 2:461–463
26. Gennaro JGJ (1969) The gecko grip. Nat Hist 78:36–43
27. Glassmaker NJ, Jagota A, Hui CY, Kim J (2004) Design of biomimetic fibrillar interfaces: 1. Making contact. J R Soc Interface 1:23–33
28. Glassmaker NJ, Jagota A, Hui CY (2005) Adhesion enhancement in a biomimetic fibrillar interface. Acta Biomater 1:367–375
29. Hamaker HC (1937) London van der Waals attraction between spherical bodies. Physica 4:1058
30. Han D, Zhou K, Bauer AM (2004) Phylogenetic relationships among gekkotan lizards inferred from C-mos nuclear DNA sequences and a new classification of the Gekkota. Biol J Linn Soc 83:353–368
31. Hanna G, Barnes WJP (1991) Adhesion and detachment of the toe pads of tree frogs. J Exper Biol 155:103–125
32. Hansen WR, Autumn K (2005) Evidence for self-cleaning in gecko setae. Proc Natl Acad Sci USA 102:385–389
33. Henry PSH (1953) The role of asymmetric rubbing in the generation of static electricity. Br J Appl Phys S2:S31–S36
34. Hiller U (1968) Untersuchungen zum Feinbau und zur Funktion der Haftborsten von Reptilien. Z Morphol Tiere 62:307–362
35. Hinds WC (1982) Aerosol Technology: Properties, Behavior, and Measurement of Airborne Particles, Wiley, New York
36. Hora SL (1923) The adhesive apparatus on the toes of certain geckos and tree frogs. J Proc Asiat Soc Beng 9:137–145
37. Houwink R, Salomon G (1967) Effect of contamination on the adhesion of metallic couples in ultra high vacuum. J Appl Phys 38:1896–1904
38. Huber G, Gorb SN, Spolenak R, Arzt E (2005a) Resolving the nanoscale adhesion of individual gecko spatulae by atomic force microscopy. Biol Lett 1:2–4

39. Huber G, Mantz H, Spolenak R, Mecke K, Jacobs K, Gorb SN, Arzt E (2005b) Evidence for capillarity contributions to gecko adhesion from single spatula and nanomechanical measurements. Proc Natl Acad Sci USA 102:16293–16296
40. Hui CY, Jagota A, Lin YY, Kramer EJ (2002) Constraints on micro-contact printing imposed by stamp deformation. Langmuir 18:1394–1404
41. Irschick DJ, Austin CC, Petren K, Fisher RN, Losos JB, Ellers O (1996) A comparative analysis of clinging ability among pad-bearing lizards. Biol J Linn Soc 59:21–35
42. Israelachvili JN, Tabor D (1972) The measurement of Van der Waals dispersion forces in the range of 1.5 to 130 nm. Proc R Soc Lond Ser A 331:19–38
43. Israelachvili JN (1992) Intermolecular and Surface Forces, 2nd edn, Academic, San Diego
44. Jaenicke R (1998) Atmospheric aerosol size distribution, In: Harrison RM, van Grieken R (eds) Atmospheric Particles. Wiley, New York, p 1–29
45. Jagota A, Bennison SJ (2002) Mechanics of adhesion through a fibrillar microstructure. Integr Comp Biol 42:1140–1145
46. Johnsen A, Rahbek K (1923) A physical phenomenon and its applications to telegraphy, telephony, etc. J Inst Electr Eng 61:713–725
47. Johnson KL, Kendall K, Roberts AD (1971) Surface energy and the contact of elastic solids. Proc R Soc Lond Ser A 324:301–313
48. Kluge AG (2001) Gekkotan Lizard taxonomy. Hamadryad 26:1–209
49. Losos JB (1990) Thermal sensitivity of sprinting and clinging performance in the tokay gecko (Gekko gecko). Asiat Herp Res 3:54–59
50. McFarlane JS, Tabor D (1950) Adhesion of solids and the effects of surface films. Proc R Soc Lond Ser A 202:224–243
51. Menon C, Murphy M, Sitti M (2004) Gecko inspired surface climbing robots, In: IEEE International Conference on Robotics and Biomimetics, August 22–26, p 431–436
52. Northen MT, Turner KL (2005a) A batch fabricated biomimetic dry adhesive. Nanotechnology 16:1159–1166
53. Northen MT, Turner KL (2005b) Multi-scale compliant structures for use as a chip scale dry adhesive. Transducers 2:2044–2047
54. Pan B, Gao F, Ao L, Tian H, He R, Cui D (2005) Controlled self-assembly of thiol-terminated poly(amidoamine) dendrimer and gold nanoparticles. Colloids Surf A 259:89–94
55. Peressadko A, Gorb SN (2004) When less is more: experimental evidence for tenacity enhancement by division of contact area. J Adhes 80:247–261
56. Persson BNJ (2003) On the mechanism of adhesion in biological systems. J Chem Phys 118:7614–7621
57. Persson BNJ, Gorb S (2003) The effect of surface roughness on the adhesion of elastic plates with application to biological systems. J Chem Phys 119:11437–11444
58. Phipps PB, Rice DW (1979) Role of water in atmospheric corrosion, ACS Symposium Series No. 89, American Chemical Society, Washington
59. Ruibla R, Ernst V (1965) The structure of the digital setae of lizards. J Morph 117:271–294
60. Russell AP (1975) A contribution to the functional morphology of the foot of the tokay, Gekko gecko. J Zool Lond 176:437–476
61. Russell AP (1986) The morphological basis of weight-bearing in the scansors of the tokay gecko. Can J Zool 64:948–955
62. Schäffer E, Thurn-Albrecht T, Russell TP, Steiner U (2000) Electrically induced structure formation and pattern transfer. Nature 403:874–877
63. Schleich HH, Kästle W (1986) Ultrastrukturen an Gecko-Zehen. Amphib Reptil 7:141–166
64. Schmidt HR (1904) Zur Anatomie und Physiologie der Geckopfote. Jena Z Naturwiss 39:551

65. Shah GJ, Sitti M (2004) Modeling and design of biomimetic adhesives inspired by gecko foot-hairs. In: IEEE International Conference on Robotics and Biomimetics. August 22–26, p 873–878
66. Shaw PE (1923) Electrical separation between identical solid surfaces. Proc Phys Soc 39:449–452
67. Simmermacher G (1884) Untersuchungen über Haftapparate an Tarsalgliedern von Insekten. Zeitschr Wiss Zool 40:481–556
68. Sitti M (2003) High aspect ratio polymer micro/nano-structure manufacturing using nanoembossing, nanomolding and directed self-assembly, In: Proceedings of the IEEE/ASME Advanced Mechatronics Conference, July 20–24, Vol 2, p 886–890
69. Sitti M, Fearing RS (2002) Nanomodeling based fabrication of synthetic gecko foot-hairs, In: Proceedings of the IEEE Conference on Nanotechnology. August 26–28, p 137–140
70. Sitti M, Fearing RS (2003a) Synthetic gecko foot-hair for micro/nano structures as dry adhesives. J Adhes Sci Technol 18:1055–1074
71. Sitti M, Fearing RS (2003b) Synthetic gecko foot-hair for micro/nano structures for future wall-climbing robots, In: Proceedings of the IEEE International Conference on Robotics and Automation. September 14–19, Vol 1, p 1164–1170
72. Skinner SM, Savage RL, Rutzler JE (1953) Electrical phenomena in adhesion I: electron atmospheres in dielectrics. J App Phys 24:438–450
73. Stork NE (1980) Experimental analysis of adhesion of Chrysolina polita on a variety of surfaces. J Exp Biol 88:91–107
74. Stork NE (1983) J Nat Hist 17:829–835
75. Timoshenko SP, Gere JM (1961) Theory of Elastic Sstability, McGraw-Hill, New York
76. Tinkle DW (1992) Gecko. Encyl Am 12:359
77. Van der Kloot WG (1992) Molting. Encyl Am 19:336–337
78. Wagler J (1830) Naturliches System der Amphibien, Cotta'schen, Munich
79. Wahlin A, Backstrom G (1974) Sliding electrification of teflon by metals. J Appl Phys 45:2058–2064
80. Williams EE, Peterson JA (1982) Convergent and alternative designs in the digital adhesive pads of scincid lizards. Science 215:1509–1511
81. Yurdumakan B, Raravikar NR, Ajayan PM, Dhinojwala A (2005) Synthetic gecko foot-hairs from multiwalled carbon nanotubes. Chem Commun 3799–3801
82. Zimon AD (1969) Adhesion of Dust and Powder, translated from Russian by Corn M. Plenum, New York
83. Zisman WA (1963) Influence of constitution on adhesion. Ind Eng Chem 55(10):18–38.